Superelastic Response of Ni–Mn–Ga Martensite in Magnetic Fields and a Simple Model

Ladislav Straka and Oleg Heczko

***Abstract*—The irreversible and reversible straining (superplasticity and superelasticity) of the single crystal $Ni_{49.7}Mn_{29.1}Ga_{21.2}$ sample stressed compressively under a static magnetic field up to 1 T is described and successfully modeled. The sample possesses a five-layered martensitic structure at room temperature and it becomes almost fully superelastic (reversible strain close to 6%) for values of field higher than 0.3 T. The maximum sensitivity of the stress-strain curve to the magnetic field determined from the model is 6.8 MPa/T (7.2 MPa/T from measured data). Knowledge of magnetization curves of the single variant sample and stress-strain curve in zero magnetic field is sufficient to predict the stress-strain behavior in an arbitrary static magnetic field.**

***Index Terms*—Magnetic shape memory, magnetic shape memory (MSM) effect, martensite, MFIS, NiMnGa, Ni–Mn–Ga, smart alloys.**

I. Introduction

FERROMAGNETIC Ni–Mn–Ga alloys in the martensitic state are promising magnetically active materials due to the existence of a giant magnetic-field-induced strain (magnetic shape memory (MSM) effect). The mechanism of the MSM effect is the motion of the martensitic twin boundaries caused by a difference of magnetic energies between martensitic variants [1], [2]. The potential use of the alloys as actuators is often suggested in published work but other applications should not be excluded. In our work, we show the possibility of using a Ni–Mn–Ga single crystal as a magnetically controlled superelastic element and we propose a simple model of the phenomena.

II. Experiment

The composition of the alloy used is $Ni_{49.7}Mn_{29.1}Ga_{21.2}$ (the same alloy as in [3]). The room temperature structure is a five-layered modulated tetragonal martensite with structure parameters $a = b = 0.595$ nm, $c = 0.561$ nm determined by X-ray diffraction. For more detailed information about the structure of Ni–Mn–Ga alloys; see, e.g., [4]. The measured sample was a prism-shaped single crystal, cut along the $\{100\}$ faces of the parental cubic $L2_1$ structure. Dimensions of the sample were approximately $4 \times 5 \times 9$ mm^3. The experimental strain is defined as a linear deformation $\epsilon = (l - l_0)/l_0$, where l is the length of the sample and l_0 is the initial length. The maximum deformation expected after the full reorientation of the tetragonal lattice is $\epsilon_m = (c - a)/a = -5.71\%$ [4].

Manuscript received December 9, 2002. This work was supported by The Finish National Technology Agency TEKES and by the consortium of Finish companies Metso Oy, Adaptamat Oy, and Nokia.

The authors are with the Laboratory of Biomedical Engineering, Helsinki University of Technology, Espoo FIN-02015 TKK, Finland (e-mail: ladislav.straka@hut.fi; oleg.heczko@hut.fi).

Digital Object Identifier 10.1109/TMAG.2003.816164

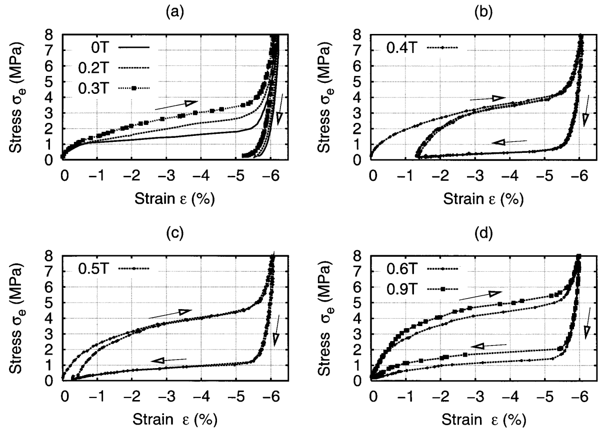

Fig. 1. Stress-strain curves for different values of the applied magnetic field. (a) For zero or small field, the sample is superplastic. (b) For a few cycles in the field of 0.4 T, the process is partly reversible. (c) Further increasing of field to 0.5 T brings more reversibility. (d) Strain is fully reversible for the field of 0.6 T and above.

The sample was placed between two heated copper plates inside a piston driven by compressed air (see inset in Fig. 2). The compressive stress was applied along the [100] crystallographic direction and the magnetic field was applied perpendicular to the stress, i.e. along the [001] direction. Sign convention is that the compressive stress is positive. The strain was measured by a laser vibrometer-dilatometer in the direction of the applied compressive stress. Magnetization in the direction of the applied field was measured using a vibrating coil magnetometer (VCM). The whole apparatus was placed inside a 12″ electromagnet. Maximum field used in the measurements was 1.1 T. The arrangement allowed us to apply stress and magnetic field and measure strain and magnetization of the sample simultaneously.

III. Results and Discussion

Stress-strain curves were measured for various fields up to 1 T. Selected curves are shown in Fig. 1(a)–(d). The magnetic field was set first and then the stress was increased from 0.2 to 8 MPa and then decreased back to 0.2 MPa. A magnetic field of 1 T was applied to the sample before each measurement to get defined state, ideally a single variant with the c-axis oriented along the field direction. Observation in polarized light showed that a small volume fraction of other variants still persisted after the field application; however these residual variants would not influence much the measurement of stress-strain curves, except for reducing the maximum possible strain. Up to 0.3 T, a relatively small external stress causes a large deformation of the sample, which is kept after stress removal (superplasticity). Above 0.3 T, the stress causes a large deformation but the original shape of the sample is recovered after stress removal (superelasticity). The higher the applied field, the higher the stress needed to compress the sample.

The large stress-induced deformation of the sample is caused by twin boundaries motion, i.e., twin variants redistribution. The external stress prefers to keep or grow variants with c-axis along the stress, while the magnetic field prefers variants with a c-axis along the field (perpendicular to the stress) [3]. Therefore, the magnetic field increases the stress needed for compressing the sample and causes the reversible deformation during unloading.

We propose a simple model to describe these phenomena, based on the model from [5]. We define the magnetic stress σ_m as the difference of magnetic energies of the martensitic variants in the external magnetic field H

$$\sigma_M(H) = \frac{\Delta E_{\mathrm{MAG}}}{\epsilon_0} = \frac{(E_{\mathrm{xEASY}} - E_{\mathrm{HARD}})}{\epsilon_0} \quad (1)$$

where $\epsilon_0 = (a-c)/c = 6.06\%$ is the distortion of the tetragonal lattice cell, and E_{EASY} and E_{HARD} are magnetic energies of the variants with the c-axis parallel and perpendicular to the field direction, respectively. The magnetic stress is fully equivalent to the mechanical stress acting along the field direction. We assume that for a given H, the magnetic stress is the same for every (properly oriented) twin boundary regardless of a distribution of martensitic variants. It implies that the internal magnetic field is the same in all variants. The true distribution of the internal field is different but the discussion of this issue is out of the scope of this article. Based on these assumptions, we can calculate the magnetic stress using the magnetization curves of the single variant sample.

To obtain the magnetization curves of a really pure single variant, the sample was heated to austenite and cooled back to martensite under compressive stress of 8 MPa. This created pure single variant with short c-axis along the compressive stress [3]. Then the magnetization curve of the variant with the c-axis perpendicular to the field was measured, still under the same stress, to prevent MSM effect. After that, the compressive stress was lowered to 0.2 MPa and strain and magnetization curves were measured, from the measurement follows that the variant with the c-axis perpendicular to the field transformed to a variant with the c-axis parallel to the field, i.e., the MSM effect occurred [1]. The value of 6.0% strain confirms that the sample switched between two single variant states. Measured magnetization curves, shown in Fig. 2, can be approximated by linear dependences

$$M_{\mathrm{EASY}} = \begin{cases} \frac{H}{H_D} M_S, & \text{for } 0 < H < H_D \\ M_S, & \text{for } H > H_D \end{cases} \quad (2)$$

$$M_{\mathrm{HARD}} = \begin{cases} \frac{H}{H_A} M_S, & \text{for } 0 < H < H_A \\ M_S, & \text{for } H > H_A \end{cases} \quad (3)$$

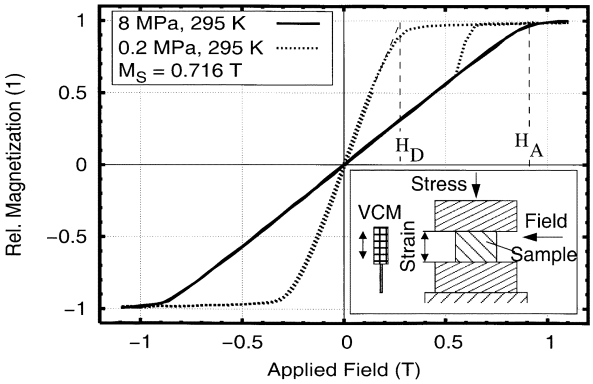

Fig. 2. Solid line shows magnetization curve of the sample constrained in single variant state measured in hard direction and dotted curve shows magnetization measurement after removing the constraint. Switching from one variant to another (MSM effect) is visible as the first-quadrant hysteresis of the dotted curve. Inset shows experimental arrangement.

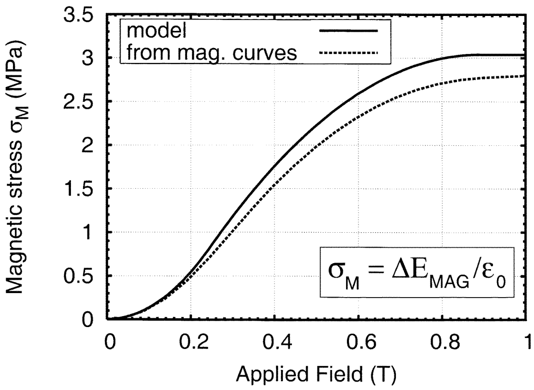

Fig. 3. Magnetic stress as a function of the applied field calculated from linearly approximated (solid line) and measured (dotted line) magnetization curves. The difference between curves is 0.2 MPa at the field 1 T.

where H is applied field, M_{EASY}, M_{HARD} are magnetizations, and M_S is saturation magnetization. H_A and H_D are the apparent anisotropy and demagnetization field. As the process is symmetrical, only $H > 0$ is taken in account. In our particular case $M_S = 0.716$ T, $H_A = 0.89$ T and $H_D = 0.25$ T. By integration of (2) and (3), we obtained the magnetic energies of the variants, and using (1) we can write

$$\epsilon_0 \sigma_M(H) = \begin{cases} \frac{1}{2} M_S H^2 \left(\frac{1}{H_D} - \frac{1}{H_A} \right), \\ \qquad \text{for } 0 < H < H_D \\ -\frac{1}{2} M_S H_D + M_S H - \frac{1}{2H_A} M_S H^2, \\ \qquad \text{for } H_D < H < H_A \\ -\frac{1}{2} M_S H_D + \frac{1}{2} M_S H_A, \\ \qquad \text{for } H > H_A. \end{cases} \quad (4)$$

The magnetic stress calculated from (4) as a function of the external magnetic field is shown in Fig. 3.

In the model the independent variable is the external stress σ_e. An additional parameter needed for the model is the twinning stress $\sigma_{\mathrm{TW}}(\epsilon, H = 0)$, defined as an external stress inducing a deformation ϵ due to the twin boundaries motion in zero field. When the sample is compressed, the external stress

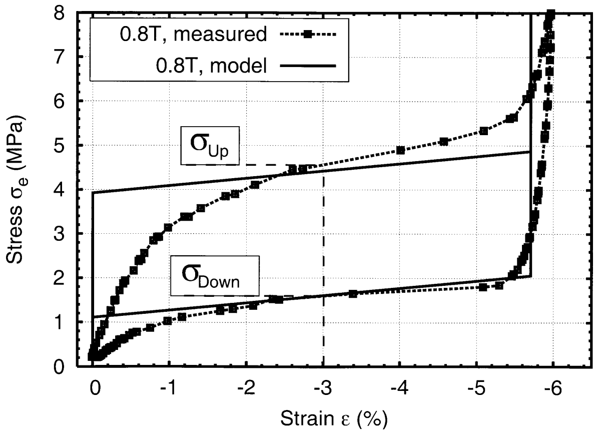

Fig. 4. Comparison of measured stress-strain curve (squares and dotted line) and model calculation (solid line) for the applied field of 0.8 T.

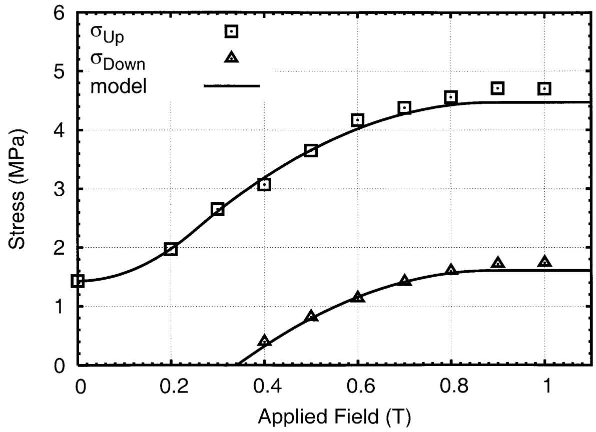

Fig. 5. External stress necessary to induce strain 3% ($\sigma_{\rm Up}$, squares) and stress induced by magnetic field at strain 3% ($\sigma_{\rm Down}$, triangles) during sample unloading as functions of the applied field. Solid line shows calculation from the model.

σ_e acts against the magnetic stress $\sigma_M(H)$ and the twinning stress $\sigma_{\rm TW}(\epsilon, H=0)$ in the direction of the external stress

$$\sigma_e = \sigma_M(H) + \sigma_{\rm TW}(\epsilon, H=0). \quad (5)$$

A different situation occurs during unloading, i.e. during sample extension, when the magnetic field (magnetic stress) acts against the external stress and the twinning stress in the direction of the magnetic field $\sigma'_{\rm TW}(\epsilon', H=0)$

$$\sigma_e = \sigma_M(H) - \sigma'_{\rm TW}(\epsilon', H=0). \quad (6)$$

Equation (6) is valid only for $\sigma_M(H) > \sigma'_{\rm TW}(\epsilon', H=0)$. We assume that $\sigma'_{\rm TW}(\epsilon', H=0) = \sigma_{\rm TW}(\epsilon, H=0)$. Due to the twinning mechanism, contraction along the field direction equals to the elongation along the direction of the external stress and thus $\epsilon' = \epsilon_m - \epsilon$. The third dimension remains constant.

Using experimental stress-strain dependence in the zero field $\sigma_{\rm TW}(\epsilon, H=0)$ [Fig. 1(a)] and experimental values H_A, H_D, M_S one can predict the stress-strain dependence $\sigma(\epsilon, H)$ for an arbitrary field H. To further simplify the model the $\sigma_{\rm TW}(\epsilon)$ dependence can be considered as linear. Comparison between a measured and a modeled stress-strain curve is shown in Fig. 4.

The agreement between the model and the measured values is excellent for the reverse process (sample unloading) for all values of the applied static field, while it is not so good for the sample compression. Fig. 1(a) shows that the presence of the applied field changes the slope of the stress-strain curve during compression. This suggests that the presence of the magnetic field changes somehow mechanism of variant nucleation and/or resistance of the structure against twin motion.

The external stress needed to obtain a 3% strain during loading ($\sigma_{\rm Up}$, see Fig. 4) and stress at a 3% strain during unloading ($\sigma_{\rm Down}$) as the functions of the applied field are shown in Fig. 5 and a comparison with the model is made.

We determined the sensitivity of the external stress on the field $S = \partial\sigma_{\rm Up}/\partial H|_{\epsilon=3\%}$ from the experimental stress-strain curves. The maximum value is about 7.2 MPa/T around $H =$ 0.2–0.3 T. This result agrees with the model which shows that the sensitivity grows up linearly from zero, it has a peak value $S_{\rm MAX} = 6.8$ MPa/T at the point $H = H_D = 0.25$ T and then it goes linearly down to zero at $H = H_A = 0.89$ T.

References

[1] O. Heczko, A. Sozinov, and K. Ullakko, "Giant field-induced reversible linear strain in magnetic shape memory NiMnGa at room temperature," *IEEE Trans. Magn.*, vol. 36, p. 3266, 2000.

[2] S. J. Murray, M. Marioni, S. M. Allen, R. C. O'Handley, and T. A. Lograsso, "6% magnetic-field-induced strain by twin-boundary motion in ferromagnetic NiMnGa," *Appl. Phys. Let.*, vol. 77, p. 886, 2000.

[3] L. Straka, O. Heczko, V. Novak, and N. Lanska, "Study of Austenite-Martensite transformation in Ni-Mn-Ga magnetic shape memory alloy," in *Proc. ICOMAT'02*, Espoo, Finland.

[4] L. Straka, O. Heczko, and N. Lanska, "Magnetic properties of various martensitic phases in Ni-Mn-Ga alloy," *IEEE Trans. Magn.*, vol. 38, p. 2835, May 2002.

[5] A. A. Likhachev and K. Ullakko, "Magnetic-field-controlled twin boundaries motion and giant magneto-mechanical effects in Ni-Mn-Ga shape memory alloy," *Phys. Lett. A*, vol. 275, pp. 142–151, 2000.